Satellite Aerodynamics and Determination of Thermospheric Density and Wind

Georg Koppenwallner

HTG Hypersonic Technology Goettingen
Max Planck Strasse 19
37191Katlenburg Lindau, Germany

Abstract. At present several satellites for earth gravity field measurement are in low polar orbits. These satellites have slender shapes and are equipped with highly sensitive accelerometer packages. Accelerometer data of these satellites can be used to determine local atmospheric density and winds. For this task accurate aerodynamic data of the satellites are required. The paper addresses how uncertainties in actual gas surface interaction and in the highly variable molecular speed ratio can be treated and minimized.

Keywords: Spacecraft, Molecular flow, Drag, Gas surface interaction, Satellite aerodynamics
PACS: 47.85Gj, 47.45.-n, 92.60hb, 94.05Hk

INTRODUCTION

A recent class of satellites designed for measuring the earth gravity field, e.g. GRACE, CHAMP and GOCE are of slender shape and equipped with highly sensitive accelerometers [1],[2],[3]. The spacecrafts are operated at low altitudes between 240 and 450 km which is necessary for accurate gravity gradient measurements. The accelerometers allow accurate measurement of the vehicles acceleration components in the body fixed reference frame. This makes these spacecraft suited for atmospheric density and thermospheric wind determination [4],[5].

Figure 1 shows the slender shape of GRACE, Champ and GOCE. The satellites are in circular near polar orbits and in nominal flight the roll-, pitch-, yaw angles are zero. The vehicle fixed x axis is pointing in flight direction and the z axis is pointing to Earth Nadir. The figure includes orbit altitude span and for GOCE the orbit plane with flight orientation.

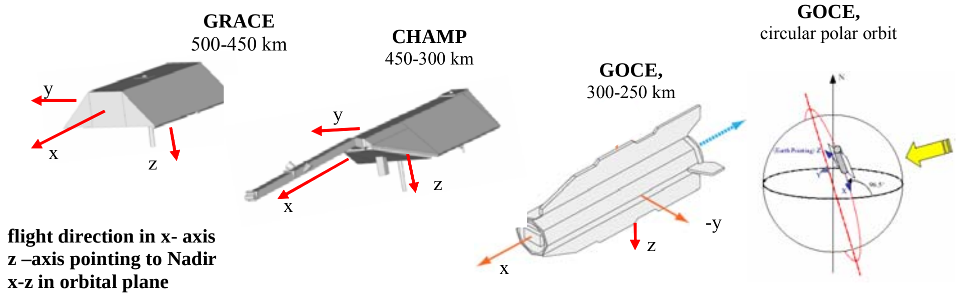

FIGURE 1. Typical gravity field explorers

Table 1 shows in more detail some orbit data, the atmospheric environment and the resulting flow conditions. Due to the slender shape of these SC the free molecular aero-force coefficients are strongly dependent on speed ratio S and actual Gas Surface Interaction GSI. Insufficient knowledge of flight speed ratio S and actual GSI impose large uncertainties on aero-coefficients, which are necessary to determine atmospheric densities and cross winds.

TABLE 1. Typical Orbit, atmospheric and flow conditions for GRACE, CHAMP, and GOCE

Quantity	GRACE	CHAMP	GOCE
Orbit, inclination	circular polar,	circular, 87.3°	circular, 96.4°
Mean altitude, km	500-400	450 - 300	300-250
Mean mol mass M, kg/kmol	15 - 16	16 - 17	15 - 19
Atmospheric temperature T, K	1800- 600	1800-600	1200-500
Mean inertial flight velocity m/s	7620	7700	7760
Mol. speed ratio S =V/c'	5.4 - 9.7	5.6 -10	5.5- 10.5
Expected flight wind angles α, β	-10° < α, β < +10°	-10° < α, β < +10°	-10° < α, β < +10°
Spacecraft mass, kg	487	522	1100
Frontal area $A_{front,}$ m^2	0.955	0.743	0.954
Area ratio $A_{parallel}/A_{front}$	15.7		28.2
Spacecraft length, m	3.1	4.288 without boom	4.915

The range of flight wind angles given in Table 1 includes side wind due to co-rotating atmosphere and due to thermospheric winds. Maximum velocity of the co-rotating atmosphere at zero latitude is 500m/s, which gives side wind angles between -3.5°< β < 3.5°

ACCELERATIONS AND AERODYNAMIC FORCES

During orbital flight the non gravitational forces acting on a satellite are aerodynamic and radiation forces. For altitudes below 400 km the solar radiation force directly acting in satellite drag contributes only with 1% to the total drag force. Thus radiation forces have only to be considered if they are acting in the vehicles y and z direction where aerodynamic forces are small.

GOCE has 6 accelerometer packages which provide 3 linear accelerations a_x, a_y, a_z. and 3 angular accelerations in body axis system. The six 3- component accelerometers are mounted symmetrically to the vehicles center of mass on the x, y, and z axis and measure continuously the linear and angular accelerations of the satellite. Forces result from aerodynamics, radiation pressure and gravitation. Aerodynamic forces and torques are below 500 km dominant against radiation and gravity gradient forces. Thus gravity gradient extraction from angular accelerations requires accurate corrections for aerodynamic and radiation forces and torques. In the following we analyze the aerodynamic aspects in order to determine air density and winds from measured linear accelerations a_x, a_y, a_z . For the aerodynamic force and moment coefficient of slender vehicles we have to consider the following dependence:

$$C_{F\,i}\;\; C_{M\,i} = \text{ Function (shape, flight wind angles } \alpha \text{ and } \beta\text{, Speed ratio S , gas surface interaction)} \qquad (1)$$

With accurate aerodynamic free molecular codes the maximum uncertainty results from insufficient knowledge of the actual speed ratio S and actual gas surface interaction. Speed ratio S is defined as V/c' and depends with c' = $(2RT)^{0.5}$ on atmospheric temperature and mean molecular mass, which are highly variable in orbital altitudes. For GSI we use the Maxwellian model with a mixed diffuse and specular reflection. The fraction of diffuse reflected molecules is given by σ, thus 1-σ gives the fraction of specular reflected particles. Using the aerodynamic force coefficients in the body fixed reference frame we obtain for the deceleration components due to aerodynamic forces:

$$ma_{x,aero} = -\tfrac{1}{2}\rho V_R^2 A_{ref} C_X(\alpha,\beta,S,\sigma,T_w) \qquad (2)$$

$$ma_{y,aero} = -\tfrac{1}{2}\rho V_R^2 A_{ref} C_Y(\alpha,\beta,S,\sigma,T_w) \qquad (3)$$

$$ma_{z,aero} = -\tfrac{1}{2}\rho V_R^2 A_{ref} C_Z(\alpha,\beta,S,\sigma,T_w) \qquad (4)$$

In this set of 3 equations are:

$a_{x,aero}$, $a_{y,aero}$, $a_{z,,aer}$	the aerodynamic acceleration components, known from measurement
m, A_{ref}	the known vehicle mass and the known reference area for aerodynamic coefficuient
$C_X(\alpha,\beta,S,\sigma)$	aerodynamic X-force coefficient calculated for ranges of (α, β, S, σ)
$C_Y(\alpha,\beta,S,\sigma)$	aerodynamic Y-force coefficient calculated for ranges of (α, β, S, σ)
$C_Z(\alpha,\beta,S,\sigma)$	aerodynamic Z-force coefficient calculated for ranges of (α, β, S, σ)
V_R	magnitude of space-craft velocity relative to co-rotating atmosphere and wind, $V_R = \|\mathbf{V_{orb}} - \mathbf{V_W}\|$ known is the orbital inertial velocity $\mathbf{V_{orb}}$,Wind vector **Vw** needs to be determined
S	Molecular speed ratio, S = V_R/c', only known with uncertainty
σ	Maxwellian Gas Surface Interaction (GSI) parameter, only known with uncertainty

The 3 equations (2, 3 and 4) must be solved for 4 quantities namely density ρ, and 3 components of the vehicles velocity vector $\mathbf{V_R}$ (v_x, v_y, v_z) relative to ambient atmosphere. One approach is to solve the equations for density ρ and aerodynamic angle of attack α and side β, which related to the vehicles velocity relative to ambient air [6]:

$$\alpha = \arctan(v_z / v_x) \quad (5)$$

$$\beta = \arcsin(v_y / V_R) \quad (6)$$

where v_x, v_y, v_z are the vehicle velocity components in body fixed reference frame relative to moving ambient air. Thus v_x, v_y, v_z include contributions from vehicles inertial velocity, from co-rotating atmosphere and from winds. As we have only 3 equations and 4 unknown quantities, a unique solution requires physically acceptable simplifications.

DRAG COEFFICIENT AND AIR DENSITY WITHOUT WINDS FOR GOCE

We assume in this case a vehicle orientation with α= β= 0°. Air density is given by the relation 7, which only requires to know the drag coefficient for the actual speed ratio S and the actual GSI parameter σ.

$$\rho = -a_{x,aero} \frac{m}{A_{ref} C_D(S,\sigma,T_w)} \frac{2}{V_{orb}^2} \quad (7)$$

Figure 2 shows the drag coefficients for a sphere and the slender GOCE shape. C_D of a sphere is almost independent on speed ratio S and the GSI parameter σ. The drag of GOCE depends strongly on speed ratio S and on the GSI parameter. GOCE drag data have been calculated with Test Particle Method of the RAMSES code system [7] and include therefore influence of molecular shielding and multiple collisions in the concave corner elements. In the GOCE drag at $S_1 \approx 10$ intersections of the $C_D(S,\sigma)$ curves are observed. At this condition the drag is independent of the GSI parameter σ . For $S_1 < 10$ a value of $\sigma < 1$ reduces C_D whereas for $S_1 > 10$ a value of $\sigma < 1$ increases C_D. Therefore at flight speed ratios S close to intersection condition an uncertainty of σ will not influence the drag.

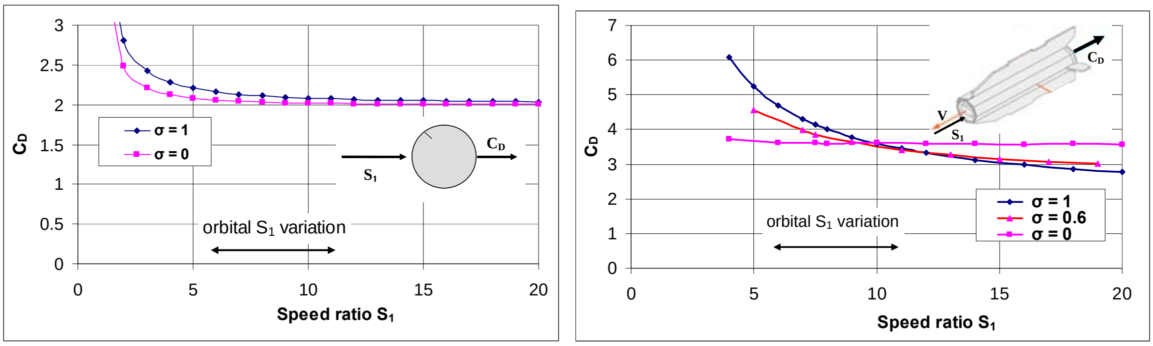

Figure 2 Drag coefficient of a sphere and the slender GOCE as function of speed ratio S_1
a. C_D of sphere with Tw/T1 = 0.3; b. C_D of GOCE calculated with Test Particle Monte Carlo method

For the design and scientific operation of low orbit scientific satellites a flight condition with low uncertainties in the C_D value can be of importance. Therefore a simple analysis shall show how this condition depends on satellite shape and flight speed ratio S. GRACE and GOCE are composed of a flat frontal area A_{front} and large lateral surfaces with zero incidence in nominal flight conditions. Thus the total drag is composed of pressure drag from frontal area and skin friction drag from flow aligned lateral surfaces. Therefore generic shapes having only frontal areas normal to flow and lateral areas parallel to flow serve in the following as test objects. CHAMP's frontal area is mainly formed by large 20° inclined front panel, it therefore does not directly fit into this generic shape class.

DRAG COEFFICIENT OF GENERIC SLENDER SATELLITE IN DEPENDENCE OF GSI AND SPEED RATIO

Typical generic body shapes with front pressure and shear stress contributions to the drag are shown in Figure 3. For these shapes we obtain a simplified drag formula (8) in which the first term represents pressure drag and the second term the skin friction drag. C_D is for all cases based on frontal area, which is normal to the flow. For speed rations S > 5 this formula agrees excellently with results by exact free molecular formulation.

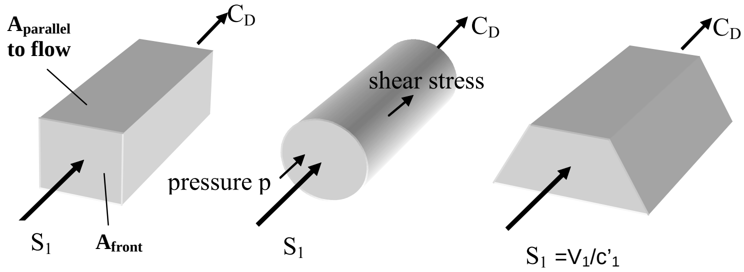

Figure 3 Generic shapes with pressure drag from front and base area plus frictional drag from lateral surfaces

$$C_D = \left(2(2-\sigma)+\sigma\frac{\sqrt{\pi}}{S_\infty}\sqrt{\frac{T_W}{T_\infty}}\right)+\frac{1}{\sqrt{\pi}}\frac{\sigma}{S_\infty}\frac{A_{Par}}{A_{front}} \qquad (8)$$

The next Figures 4a and 4b show a drag analysis of the generic bodies with A_{par}/A_{front} = 16 and 32 and with a variation of the Maxwell accommodation coefficient between σ = 0 and 1. Each figure shows one common intersection point, at which the drag coefficient is independent from the accommodation parameter σ. The intersection occurs in each case at the same value of C_D = 4 given for specular reflection. With increasing A_{par}/A_{front} the intersection is shifted to higher speed ratios S_{int}. Thus an uncertainty of the accommodation value σ acts in the following way: For $S < S_{int}$ the drag increase with increasing σ and for $S > S_{int}$ a drag decreases with increasing σ.

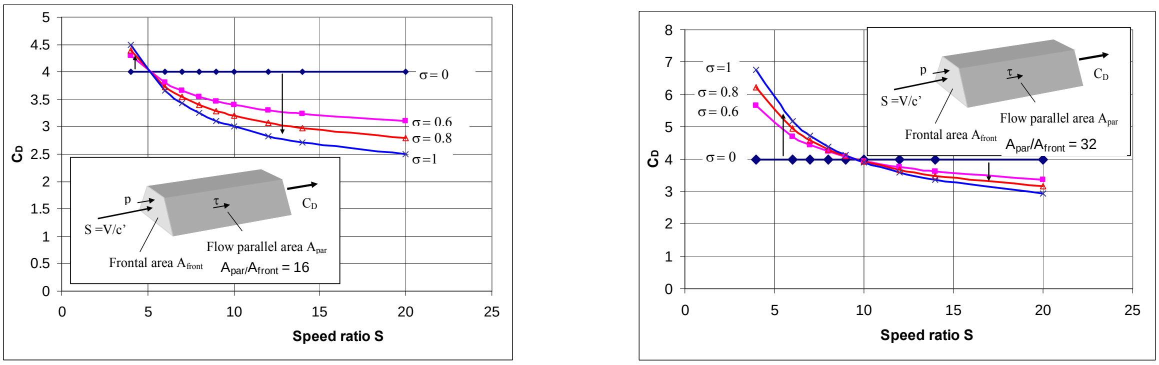

Figure 3 CD as function of speed ratio S for = 1, 0.8, 0.6 and 0 ; a: A_{par}/A_{front} = 16; B. = A_{par}/A_{front} = 32

To derive a drag coefficient sensitivity on σ we take the derivatives of the C_D formula with respect to the accommodation coefficient σ. For the $dC_D/d\sigma$ and for the condition $dC_D/d\sigma = 0$ we obtain:

$$\frac{dC_D}{d\sigma} = -2+\frac{1}{S_\infty}\left(\sqrt{\pi}\sqrt{\frac{T_W}{T_\infty}}+\frac{1}{\sqrt{\pi}}\frac{A_{par}}{A_{front}}\right) \quad \frac{dC_D}{d\sigma}=0 \;\; for\; S_{\text{int}} = \frac{1}{2}\left(\sqrt{\pi\frac{T_W}{T_\infty}}+\frac{1}{\sqrt{\pi}}\frac{A_{par}}{A_{front}}\right) \qquad (9a,b)$$

The C_D value for zero sensitivity is unique and given by S_{int} and the drag formula 8.

C_D *for* $dC_D/d\sigma = 0$: $\quad C_D = 2(2-\sigma) + 2\sigma = 4$ (10)

Using equation 9b we can define the regions of neutral positive and negative drag sensitivity with respect to a σ change. Figure 4 shows these regions in a plot of speed ratio S versus A_{par}/A_{front}.

In the Maxwell model the vehicle is exposed to a stream of diffusely and to a stream of specularly reflected particles. Both parts are leaving the SC without mutual interaction and therefore the following linear relation holds for the drag coefficient composition.

$$C_D = \sigma C_{D,diffuse} + (1-\sigma)C_{D,specular} \qquad (11)$$

As the diffuse reflection with σ = 1 is usually observed for technical surfaces we are interested on the possible drag deviation from this case. We therefore use a normalized drag sensitivity with respect to C_D at diffuse reflection.

$$\frac{\Delta C_D}{C_{D,diffuse}} = \frac{C_D(\sigma)-C_D(\sigma=1)}{C_D(\sigma=1)} = (\sigma-1)+(1-\sigma)\frac{C_{D,specular}}{C_{D,diffues}} \qquad (12)$$

To evaluate this equation one needs in principle drag calculations for σ = 0, σ = 1 and for the expected maximum and minimum speed ratios S_{max} and S_{min} during orbital flight. If we postulate an uncertainty span of σ between 0.6 < σ < 1 we obtain normalized drag errors as shown in Fig. 4b.

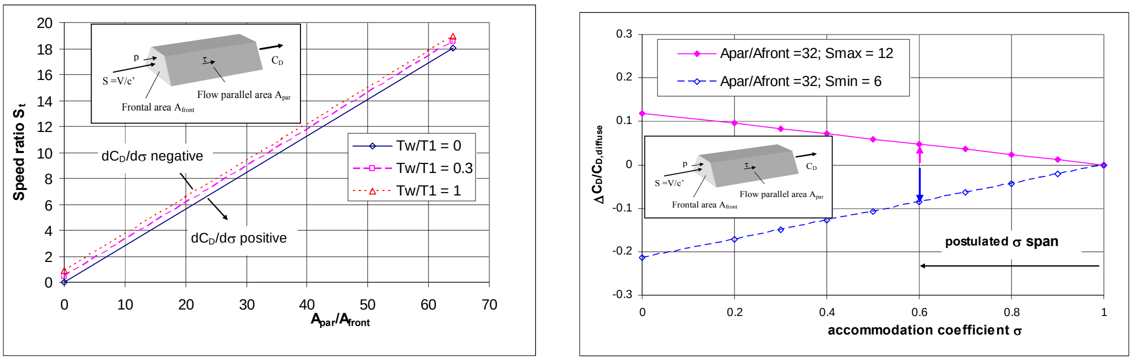

Figure 4 a Conditions for neutral, positive and negative drag sensitivity on accommodation coefficient; b Drag coefficient sensitivity on accommodation coefficient σ for $A_{par}/A_{front} = 32$

LATERAL SIDE WIND DETERMINATION AND AERODYNAMICS

We use as example CHAMP and postulate that body fixed axis system is nominally aligned in the orbit plane. Lateral side wind produces in this case at α = 0 a side wind dependent side slip angle β. As accelerations are measured in body axis system we need axial force and lateral force as function of side slip angle β. We use equations 2 and 3 and obtain the following relation between side-slip angle β and accelerations in x and y direction. If aerodynamics provides one function for the force ratio functional dependence is further simplified.

$$\frac{a_{y,aero}}{a_{x,aero}} = \frac{C_Y(\alpha = 0, \beta, S, \sigma, T_w)}{C_X(\alpha = 0, \beta, S, \sigma, T_w)} = \frac{C_Y}{C_X}(\alpha = 0, \beta, S, \sigma, T_w) \qquad (13)$$

This relation is independent of vehicle mass, reference area and atmospheric density and needs to be solved for the slip angle β. Figure 5 shows the dependence of C_Y, C_X and C_Y/C_X on β for different speed ratios S. For the mean speed ratio of S = 7.5 similar results are shown in Figure 6 for different gas surface interaction parameters Figure 6. All aerodynamic data have been calculated with the Test Particle Method (TPMC) of the RAMSES/ANGARA code [7] using a finely meshed surface of CHAMP. By use of the force ratio C_Y/C_X we have created a quantity related to sideslip angle β with reduced dependence on speed ratio S and GSI parameter σ.

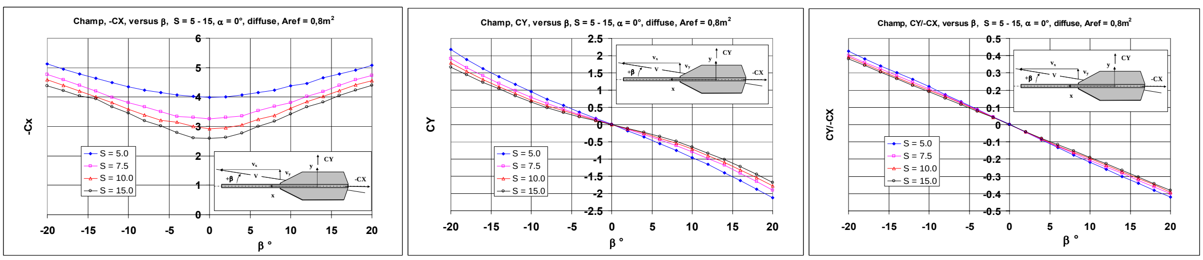

Figure 5 CHAMP C_X ,C_Y force coefficients and C_y/C_X ratio versus β slip angle for different speed ratios S

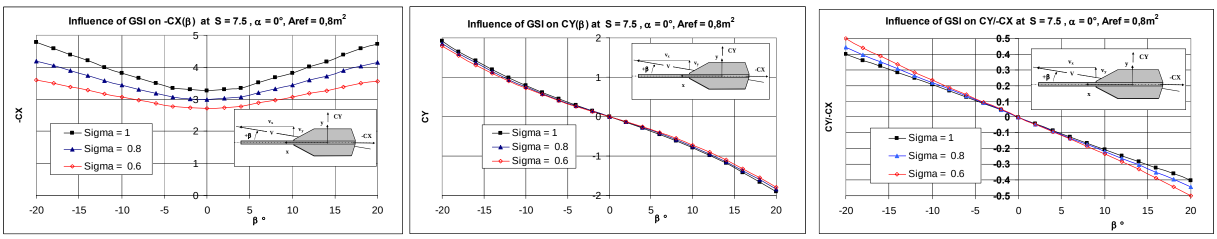

Figure 5 Champ C_X ,C_Y force coefficients and C_y/C_X ratio versus β for GSI values of σ =1, 0.8 and 0.6

For the parameter range of 5 < S < 10 , 0.6 < σ < 1 and side slip angles between -10°<β< 10° we observe a linear dependence of (C_Y/C_X) on β, with a small influence of S and σ on the slope. For side wind determination we thus can use the linear derivative d(CY/CX)/dβ. The d(CY/CX)/dβ derivatives for selected speed ratios S and GSI parameters σ are shown in Table 2 and 3. For error analysis the references have been taken at S = 7.5 and σ = 0.8.

TABLE 2. Beta derivative of CY/CX in speed ratio range S = 5-10 α = 0°, σ = 1

Speed ratio S	d(CY/CX)/dβ, 1/°	Deviation to reference, %
5	0.0214	5.58
7.5 (reference)	**0.0202**	0.00
10	0.0196	-3.11

TABLE 3. Beta derivative of CY/CX for σ = 0.6, 0.8 and 1, S = 7.5 α = 0°

Accommodation σ	d(CY/CX)/dβ, 1/°	Deviation to reference, %
0.6	0.0235	6.33
0.8 (reference)	**0.0221**	0.00
1	0.0209	-5.43

The tables show that the derivative d(CY/-CX)/d β is in the selected range almost independent on speed ratio and gas surface interaction. Deviations to reference values are in the range between -5.43 and 6.33%. If this accuracy is accepted equation 13 could be replaced by a formulation with static derivative and directly be solved for the sideslip angle *β*.

$$\frac{a_{y,aero}}{a_{x,aero}} = \frac{d(C_Y / C_x)}{d\beta}\beta \quad \text{or} \quad \beta = \frac{a_{y,aero} / a_{x,aero}}{d(C_Y / C_x)/d\beta} \tag{14}$$

If higher accuracy is required only a speed ratio dependence of d(CY/-CX)/dβ should be included. In view of the existing physical uncertainty of gas surface interaction the proposed reference value for σ = 0.8 seems adequate. It has to be noted that the accuracy of force and moment derivatives at α= β= 0 depends strongly on the analysis method. For spacecraft with concave corner elements like GOCE only the TPMC method gives reliable results

CONCLUSIONS

Air density and wind derivation from multiaxis accelerometer data on satellites is an inverse problem and requires in principle a detailed aerodynamic analysis. It has been shown how uncertainties due to gas surface interaction and the speed ratio S can be assessed and minimized. For GOCE and CHAMP type shapes an optimum ratio of lateral to frontal area can be derived for a mean operational speed ratio. At this condition drag is independent of Maxwellian gas surface interaction parameterσ . For side wind determination an aerodynamic analysis approach using derivatives of the relevant force ratios offers distinct advantages.

REFERENCES

1. Ch. Reigber, H. Luehr, P. Schwintzer, *CHAMP mission status*, Advances in Space Research, 30(2), 2002, pp.129–134,
2. J. Flury, S. Bettadpur, B. D.Tapley, *Precise accelerometry onboard the GRACE gravity field satellite mission*," Advances in Space Research, Vol. 42, No. 8, 2008, pp. 1414-1423.
3. M. Fehringer, G. Andre, D. Lamarre, D. Moeusly, *GOCE and its Gravity Measurement Systems,* ESA-Bulletin No.133, European Space Agency, Noordwijk, Netherlands, 2008, pp.15-23
4. Sutton, E. K., Nerem, R. S., and Forbes, J. M., *Density and winds in the thermosphere deduced from accelerometer data,* Journal of Spacecraft and Rockets, Vol. 44, No. 6, 2007, pp. 1210-1219.
5. E. Doornbos et alea. *Neutral Density and Crosswind Determination from Arbitrary Oriented Multiaxis Accelerometers Satellites,* Journal Spacecraft and Rockets, 2010 (accepted for publication)
6. Anonym, *Recommended Practice for Atmospheric and Space Flight Vehicle Coordinate Systems*, AIAA Washington, 1992. ANSI/AIAA R004-1992
7. G. Koppenwallner, D. Johannsmeier, H. Klinkrad, M. Ivanov, A Kashkowski *A Rarefied Aerodynamics Modelling System for Earth Satellites, (RAMSES),* in 'Rarefied Gas Dynamics', Vol.2 , Ed. J. Harvey, G. Lord, Oxford University Press, Oxford 1995, pp. 1366-1372.

Satellite name explanations: GRACE Gravity Recovery and Climate Experiment
CHAMP CHAllenging Mission Payload
GOCE Gravity field and steady state Ocean Circulation Explorer